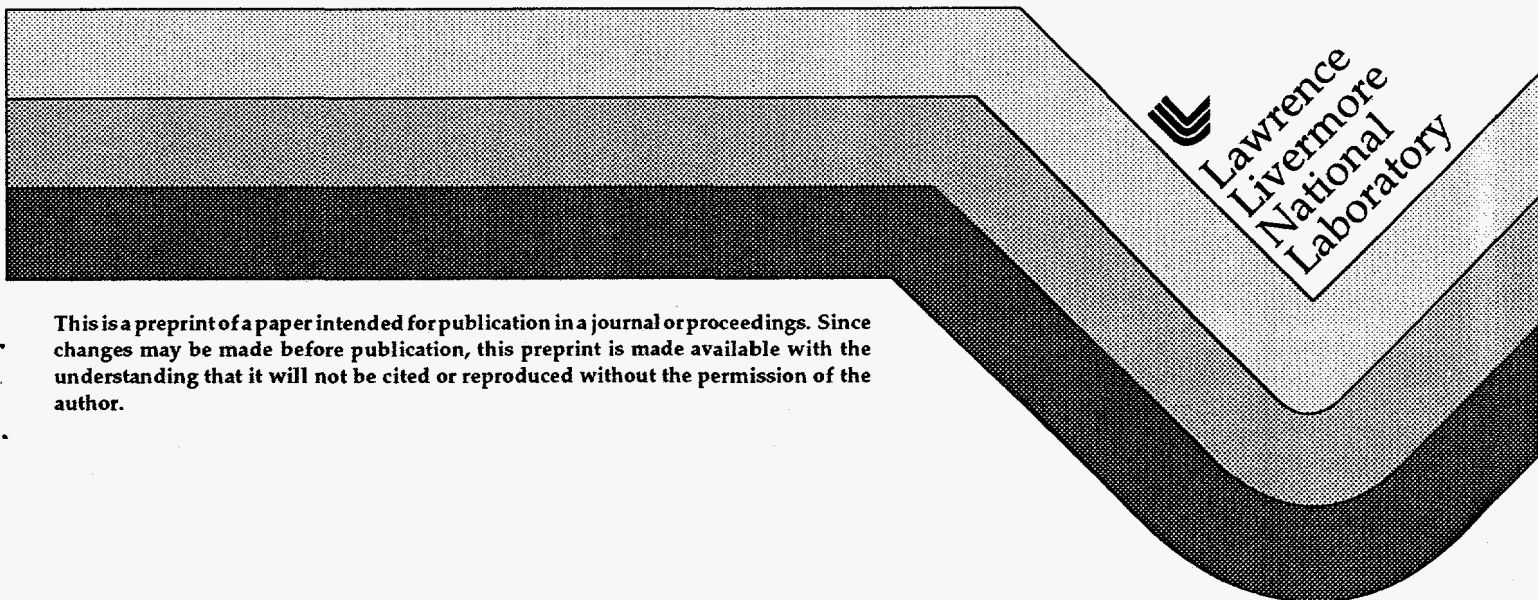# Molecular Dynamics Simulation of Mechanical Deformation of Ultra-Thin Metal and Ceramic Films

J. Belak
J.N. Glosli
D.B. Boercker
I.F. Stowers

This paper was prepared for submittal to the
Materials Research Society
San Francisco, CA
April 20, 1995

April 1995

Lawrence
Livermore
National
Laboratory

DISCLAIMER

DISCLAIMER

Portions of this document may be illegible in electronic image products. Images are produced from the best available original document.

MOLECULAR DYNAMICS SIMULATION OF MECHANICAL DEFORMATION OF ULTRA-THIN METAL AND CERAMIC FILMS

J. BELAK, J.N. GLOSLI, D.B. BOERCKER, and I.F. STOWERS
University of California, Lawrence Livermore National Laboratory, Livermore, CA 94550

ABSTRACT

We present an overview of the molecular dynamics computer simulation method as employed in the study of the mechanical properties of surfaces at the nanometer scale. The embedded atom method is used to model a clean metal surface and the bond-order model is used to model ceramic surfaces. The computer experiment consists of the indentation and scraping of a hard diamond-like tool into and across the surface. Results are presented for the (111) surface of copper and silver and for the (100) surface of silicon. We explicitly demonstrate in our point indentation simulations that nanoscale plasticity in metals takes place by nondislocation mechanisms, a result suggested by recent nanoindentation experiments. We also observe the surface to accommodate nearly the entire volume of the tip and the annealing out of plastic work as the tip is removed. In our orthogonal cutting simulation, we observe an interesting phenomenon: the system dynamically reorients the grain in front of the tool tip to minimize the work performed on the shear plane (i.e. the shear plane becomes an easy slip plane). Silicon transforms into an amorphous state which then flows plastically.

INTRODUCTION

The precision machining of metal surfaces and the ductile-regime grinding of ceramic surfaces are examples of fundamental cutting processes utilized in the fabrication of high-tolerance parts. Components with dimensional tolerances of a few tens of nanometers can currently be produced by direct machining. Despite the ability to fabricate these parts, little is understood of the basic deformation mechanisms that determine how material is removed and deformed, how a tool-tip and workpiece interact, how induced surface and subsurface damage occur, and how cutting tools wear. For example, the wear rate of single-point diamond tools is extremely rapid when silicon or ferrous materials are machined [1]. This tool wear is the limiting factor in the resulting contour accuracy and surface finish quality.

The key to solving these problems is a fundamental understanding of basic tribological processes such as surface indentation and scraping. For example, controlled surface indentation experiments are an important tool in the study of surface deformation [2]. A hard, sharp tool is used and the effort required to indent a surface is measured. The primary observable is the material hardness (H). Quantitatively, hardness is the normal load divided by the contact area projected onto the surface plane. Macroscopic experiments (indents much larger than the material grain size) indicate that, for fully plastic indents, the hardness is about three times the observed tensile yield strength (Y). Many years ago, Heinrich Hertz developed a successful theory of contact mechanics based on continuum elasticity [3, 4]. From the measured bulk elastic properties (E, v, G,...), the Hertzian theory predicts the area of contact and the stress and strain fields for a given applied normal load. We have recently verified that this theory is valid down to the nanometer length scale as long as the material remains elastic [5]. Departure occurs when the material yields plastically, as may be expected.

The surface indentation technique has been extended to the sub-micrometer length scale in order to study material deformation within a single grain. In the pioneering work of Gane and Bowden [6], a very sharp tip (diameter ~ 100 nm) was pressed into the surface of a metal crystal. They observed an interesting phenomenon—no permanent penetration occurred until a critical load was reached. Furthermore, the load at critical yielding corresponded to the theoretical shear strength of the metal. Critical yielding of this type has since been observed by many investigators [7] and, as we shall see, is also observed in the molecular dynamics simulations presented here. Chen and Hendrickson [8] used the microindentation technique to study the dynamics of dislocation creation and motion on the (111) surface of silver crystals. They were able to demonstrate the presence of dislocations on the surface by chemically etching the surface after performing the microindentation experiment. The surface preferentially etches along the edge of a dislocation loop (where the atoms are the furthest from equilibrium) and forms pits where the dislocation loop emerges at the surface. These pits form a hexagonal "rosette" pattern reflecting the symmetry of the (111) surface. More recently, Pharr and Oliver [9] have extended the experiments on the silver (111) surface using a nanoindenter (nanometer resolution along the vertical axis) and have found some rather interesting results. Hardness tends to increase with decreasing depth of indentation and the dislocation rosette patterns disappear entirely at very shallow indentations (< 50 nm), suggesting that very small scale indentation plasticity takes place by non-dislocation mechanisms. In this paper we present direct molecular dynamics evidence of this assertion—dislocations are not an efficient mechanism for accommodating strain due to point indentations at the nanometer length scale.

Probably, the most useful tool to date for the study of the mechanical properties of surfaces at the nanometer scale is the atomic force microscope (AFM) [10]. The diameter of an AFM tip can be less than 10 nm. Though several important studies of atomic scale tribological processes using the AFM have appeared [11, 12, 13], several important issues concerning the interpretation of the observed forces remain [14, 15]. In particular, the role of water vapor and other adsorbed films (especially oxide layers) is unknown and few, if any, experiments have been performed in ultra-high vacuum. It is with the aim of understanding and providing a model for the mechanics and mechanisms of tip-to-surface interactions that several molecular dynamics and atomistic studies have appeared. In the pioneering work of Landman and coworkers [16, 17], the indentation of a sharp metallic tip into a metal surface was simulated and they observed an interesting effect. Beneath a critical separation, the atoms in the tip and surface "jumped-to-contact," forming a neck between the tip and surface. This "avalanche in adhesion" had previously been predicted for planar contacts using the Lennard-Jones force model [18] and the equivalent crystal force model [19].

In the present paper we present the results of a molecular dynamics study of the indentation and orthogonal cutting of the copper and silver (111) and silicon (100) surfaces by a hard diamond-like tool.

MOLECULAR DYNAMICS MODELING

The molecular dynamics (MD) computer simulation method [20] is an ideal tool for studying the mechanics and mechanisms by which very small indents are produced and material is removed at the nanometer length scale. During these simulations, we evaluate the response of a material subjected to an external force by following the response of every atom in the material. In practice, we calculate the force on each atom in the system due to its neighbors and advance the positions with a finite difference integration scheme.

A revolution has occurred during the past decade in our understanding of empirical interatomic force models. The interatomic force is assumed to be derivable from a total potential
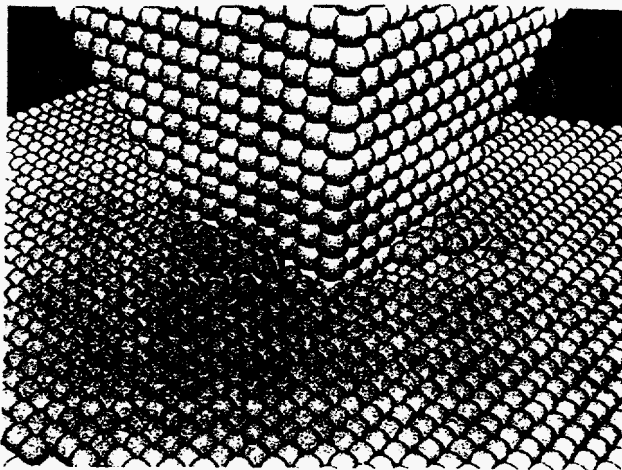
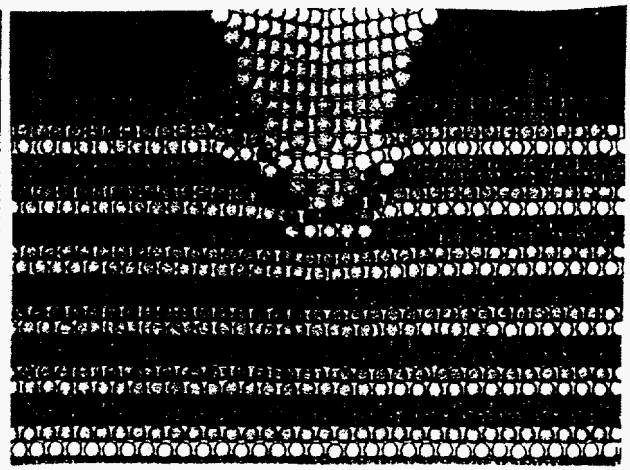Figure 4. The simulation in Figure 2 at an indentation of 7 layers.

Figure 5. A cross-section showing atoms shaded by their initial depth..
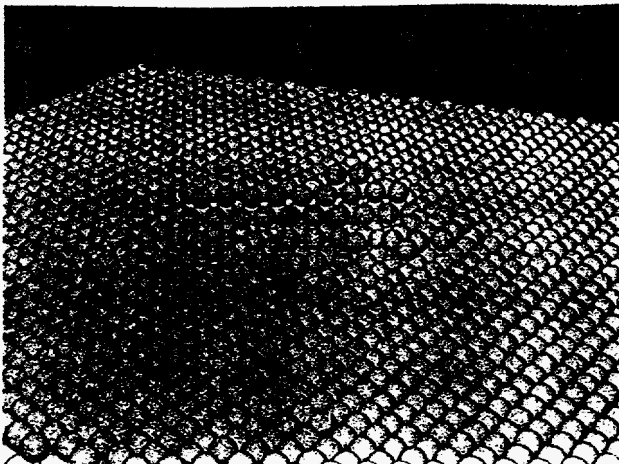

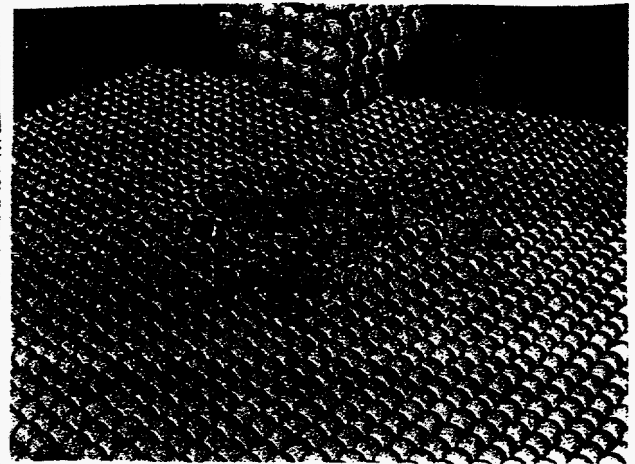Figure 6. The resulting indent and pile-up after indenting at 1 m/s.

Figure 7. The resulting indent and pile-up after indenting at 10 m/s.

elastically. The magnitude of the force is reasonable when compared to recent AFM studies [14, 15]. After an indentation of about 1.5 layers (1 layer ~0.25 nm), the surface yields plastically and the load drops significantly. This critical yielding is reminiscent of that observed in the laboratory [6]. For this simulation, the first yielding event corresponds to a single atom "popping" out onto the surface from beneath the tool tip. Upon further indentation, the system undergoes several of these loading/unloading events. After an indentation of nearly seven layers, we reverse the direction of the tool and observe the load to quickly drop to zero. However, upon further removal, the load suddenly rises again. Presumably, some plastic event has annealed at the surface, the material has returned to more intimate contact with the tool and the load rises.

In these simulations, we observe two primary mechanisms of plastic deformation; atoms popping out onto the surface and atoms being pressed into interstitial positions. Figure 4 illustrates the pile-up of atoms around the tool tip at an indentation of nearly seven layers. We note that the volume of material on the surface in no way accounts for the volume of the tip beneath the surface—through elastic and plastic deformation the surface has accommodated nearly the entire volume of the tip! We also note, in Figure 4, what appears to be dislocations beginning to emerge

on the surface near the right hand edge of the tip and on the left hand side in front of the tip. These dislocations do not extend more than a few lattice spacings. This is more clearly illustrated in Figure 5, where we show a cross-sectional slice through the center of the tip for the indentation shown in Figure 4. The atoms have been shaded according to their initial depth into the material. The shading pattern repeats every four layers. We have found this technique useful in our two dimensional simulations of the indentation process. The passage of a dislocation edge causes a mismatch between successive layers and the shading highlights the dislocation path so that it is easily discernible to the eye. We have made many cross-sectional plots like this and they all indicate that the range of plastic deformation is limited to at most a few lattice spacings surrounding the tool tip—we do not observe any dislocations. Figure 6 is an image of the indent after the tool has been removed. The volume of the indent is exactly accounted for by the pile-up on the surface. Figure 7 is a similar image taken at the end of our computer experiment at 10 m/s. The step on the surface in front of the indent demonstrates the presence of a small dislocation loop extending into the surface to the bottom of the indent. The same type of dislocation we see beginning to emerge in Figure 4. Clearly, there is a rate dependence. At the faster rates, the material does not have time to completely respond elastically and, in order to release the large build up of elastic energy in the small region around the tip, the system responds by plastically deforming, much like a mode-II fracture.

Orthogonal Cutting of the Copper (111) Surface

Over the past few years, we have developed a highly successful MD model [30] of the orthogonal cutting process [31]. The simulations were performed in two dimensions (2D) in order to achieve the length scales and time scales commonly employed in the laboratory using state-of-the-art single-point diamond turning machines. Our calculated cutting forces are in remarkable agreement with experiment [32]. In light of the above results on the point indentation of metal surfaces, this agreement seems somewhat fortuitous. In the 2D simulations, dislocations are readily created and propagate many hundred lattice spacings throughout the material. These 2D dislocations are pure edge dislocations and the work required to move them is independent of the distance from the source. In 3D, however, the dislocation forms a loop and the work required to move the dislocation is proportional to the loop length which increases with distance from a point source [29].

Shown in Figure 8 is an image of the system taken during our simulation of the orthogonal cutting process. The rake face of the tool is cleaved along the (111) plane in the cubic diamond lattice. The clearance face is generated by cleaving at an angle of about 10 degrees relative to the normal to the rake face. Atoms are systematically removed from the tip to make a tip radius of about 2 nm. The geometry of the work material is the same as the indentation simulation described above. We employ the periodic boundary condition along the y-axis and our constant velocity boundary condition along the x and the z axes. All atoms within the boundary regions on the bottom, left hand and right hand sides (see Figure 1) are constrained to
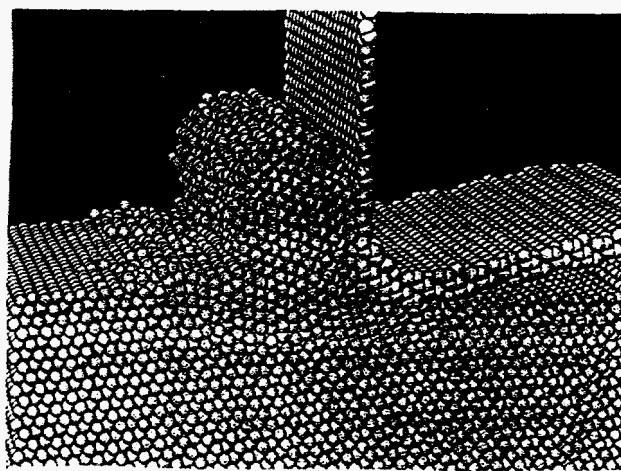

Figure 8. MD simulation of the orthogonal cutting of copper.

energy function, which in turn is a function of the positions of all of the atoms. The traditional approach has been to expand the total potential energy into terms that depend on the coordinates of a single atom (possibly due to an externally applied field), terms that depend on the coordinates of two atoms (the pair potential), and higher order terms that depend on the coordinates of many atoms. Such an expansion has proved extremely successful in the study of rare gases and molecular crystals [21], where pair interactions dominate. These models, however, fail to describe the cohesion of simple metals and covalent materials, which are of practical interest. In particular, vacancy formation and free surfaces are poorly represented.

The new approach is to develop a model of cohesion. One such model that has been enormously successful in describing the properties of simple metals is the embedded-atom method (EAM) [22]. The total potential energy is expressed as a sum of two-body interactions between the atoms and an energy required to embed each atom into the local electron density. This density is a superposition of densities localized on neighboring atoms. In this work, we employ the EAM potential parameters due to Oh and Johnson [23]. This model is based upon an exponential two-body repulsion and includes interactions out to third nearest neighbor (42 neighboring atoms).

Another model of cohesion that is currently revolutionizing MD simulations is the bond-order model due to Tersoff [24]. The strength of the attractive interaction between an atom and its neighbor is assumed to decrease with the number of nearest neighbors that atom is bonded to (the bond-order). This model provides a realistic description of cohesion in strongly covalent solids such as silicon and carbon. We employ this model in our simulations of silicon and its extension by Brenner [34,35] in our simulations of carbon.

TRIBOLOGICAL BOUNDARY CONDITIONS

By its very nature, any numerical solution of Newton's equations of motion must be for a finite number of atoms, though techniques such as periodic boundary conditions may be used to model a sub-system embedded within a much larger system. Systems as large as a few million atoms have been simulated on currently available computers. However, there is a trade-off between the number of atoms and the period of time simulated. In this work we employ no more that 10^5 atoms in order to simulate periods of time as long as a few nanoseconds. The equations of motion are integrated by approximating the time derivative by a central difference [25], with a time-step (Δt) of about 1/25 of the interatomic vibrational period (τ_E), where $\tau_E \approx 0.3$ picoseconds for copper at room temperature.

Figure 1. A schematic illustration of the boundary conditions used in our molecular dynamics simulations.

The cartoon in Figure 1 illustrates the boundary conditions used in our MD simulation of tribological problems. The boundary atoms at the top and the bottom of the simulation cell are fixed (not allowed to vibrate). These atoms serve as handles to position the tool relative to the surface. The boundary atoms at the sides of the simulation cell are either fixed (as in our constant velocity boundary condition) or periodic. Next to the fixed boundary, we place a region of thermostat atoms. A time dependent viscous damping is added to the equation of motion for these
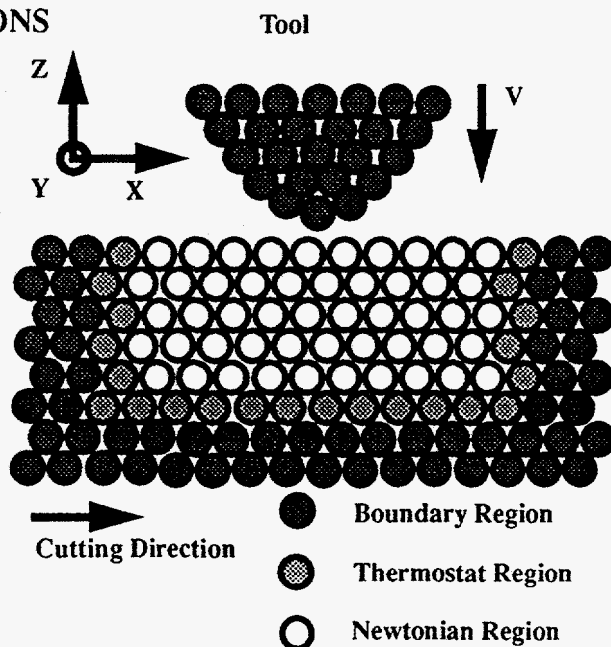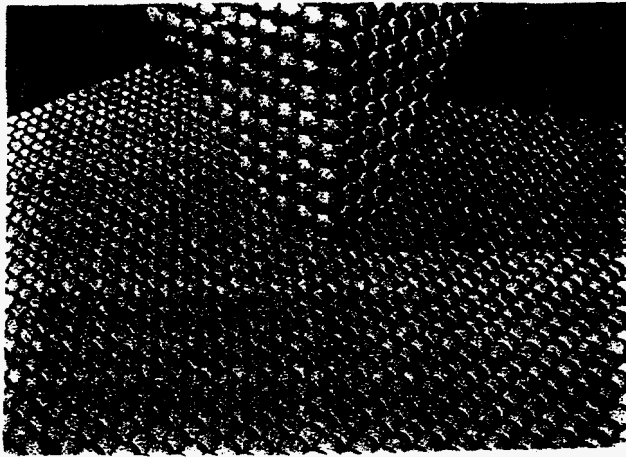
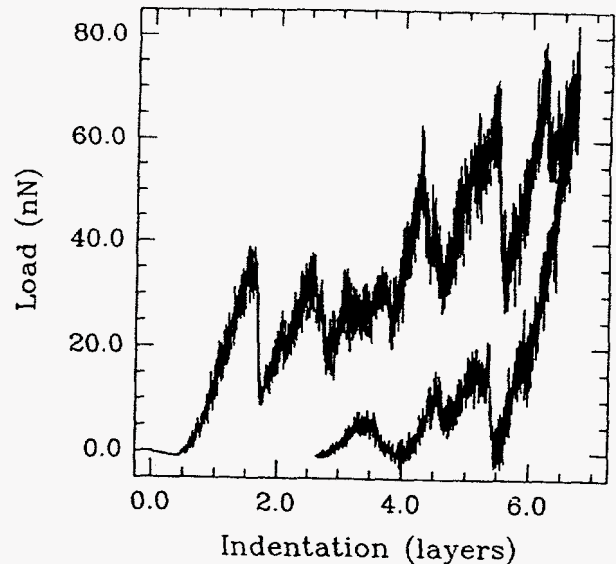Figure 2. MD simulation of copper surface indentation. The surface contains 72,576 atoms in 36 layers.

Figure 3. The loading curve for the simulation in Figure 1.

atoms [26, 27]. The purpose of these atoms is to draw away heat produced by doing work at the tool tip. In all of the simulations presented here, the thermostat is held at room temperature (300K) and all of the surfaces are fully equilibrated prior to starting the indentation. During the simulation, the remaining surface atoms are free from further constraint.

We model the diamond tool as infinitely hard—the simulated carbon atoms do not vibrate. The interaction between the atoms in the surface and the carbon atoms in the tool is via a Lennard-Jones potential model [28] with the well depth determined by the van der Waals attraction between the two surfaces.

RESULTS

Indentation of the Copper (111) Surface

Shown in Figure 2 is an image of our system taken at the start of the simulation. We employ a rigid lower boundary and a periodic boundary condition within the plane of the surface. The computer experiment consists of moving the tip into the surface at a constant velocity and observing the response of the surface atoms. We have performed the indentation at 1, 10, and 100 m/s. Faster rates are comparable to the material sound speed and, hence, do not allow sufficient time for the surface to relax. Nanoindentation experiments are performed in the laboratory at much slower rates, as slow as 10^{-6}-10^{-9} m/s [9, 14, 15]. Rates as slow as this are beyond the current capabilities of MD simulations and we are unable to study as yet plastic deformation due to phenomena such as creep and solid-state diffusion.

Our tip is very sharp. We generate the tip by cleaving along three {111} planes in the cubic diamond structure. The tip-most atoms are systematically removed to make the blunted tip as shown in Figure 2. The carbon atoms in the tip do not vibrate and we allow for no reconstruction of the diamond surface. The interaction between the carbon atoms and the copper atoms in the surface is expressed as a Lennard-Jones potential with parameters chosen to describe the weak van der Waals adhesion between the two surfaces. The instantaneous load (normal force) on the tool as a function of indentation at a rate of 1 m/s is shown in Figure 3. The upper portion of the curve is the load during indenting into the surface and the lower portion is the load during removal. After the initial van der Waals attraction, the load rises linearly as the surface responds

propagate in the +x direction at the cutting speed (100 m/s). The incoming boundary region is two lattice spacings thick and each time the material has moved one lattice spacing an entire new plane of material is inserted, producing a steady-state flow. Atoms that leave the simulation cell are discarded—the system is open. The computer experiment consists of indenting the tool into the surface at one fifth of the cutting speed while the material beneath flows past. We stop the indentation at a depth of cut of about 1 nm.

The resulting forces on the tool as a function of time are shown in Figure 9. The cutting force is the force per unit width in the direction of cut (the x-axis). For early times (prior to the surface yielding plastically), the cutting force displays large positive and negative oscillations reflecting the atomic structure of the undeformed surface. The period of these oscillations equals the time taken in moving the surface one lattice spacing at the cutting speed. When the surface yields plastically at t ~0.025ns, the cutting force increases sharply and rises only slightly during further indentation, finally achieving a plateau of F_c ~0.009 N/mm at the depth of cut of 1 nm.

Figure 9. (a) The thrust force per unit width versus time for the simulation shown in Figure 8. (b) The cutting force per unit width versus time.

The thrust force per unit width, for time less than 0.05 ns, displays a behavior reminiscent of the load per unit width during our indentation simulation. After t ~0.05 ns, we turn off the indentation and the thrust force drops significantly as we unload the clearance face. The thrust force has not reached a steady-state value over the time period of this simulation. There are long time scale events (>1 ns) associated with the cutting process (a behavior we find in our 2D simulations as well [32]) and an accurate determination of the forces demands an average over many of these events.

The image of the system in Figure 8 displays some interesting phenomena. There is a dislocation running into the surface on the right hand side of the figure and the chip is crystalline with a different orientation than the surface. This effect is more clearly illustrated in Figure 10. This figure is a projection of the atomic coordinates, from the state shown in Figure 8, onto the x-z plane. The size of the circles used to represent the atoms is much smaller than the atomic radii. Probably the most startling feature of this figure is that circles for successive layers (there are 20 layers in this simulation) lie on top of one another. This is a consequence of the simulation temperature (300 K) being much less than the melting temperature of copper (~1300 K), hence the amplitude of atomic motion about a lattice site is relatively small. The figure displays several other interesting phenomena. There is a region of high disorder immediately in front of the tool tip and another in front of the chip. There is a low angle grain boundary running between these two disordered regions with a twin boundary in the middle of the new grain. The crystalline structure of the chip is clearly illustrated and there is appreciable disorder within the lattice planes run-
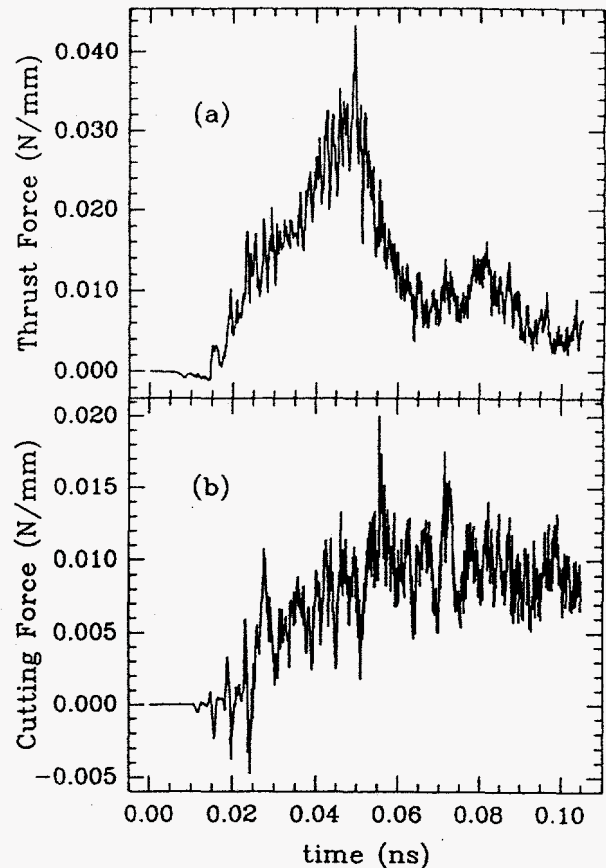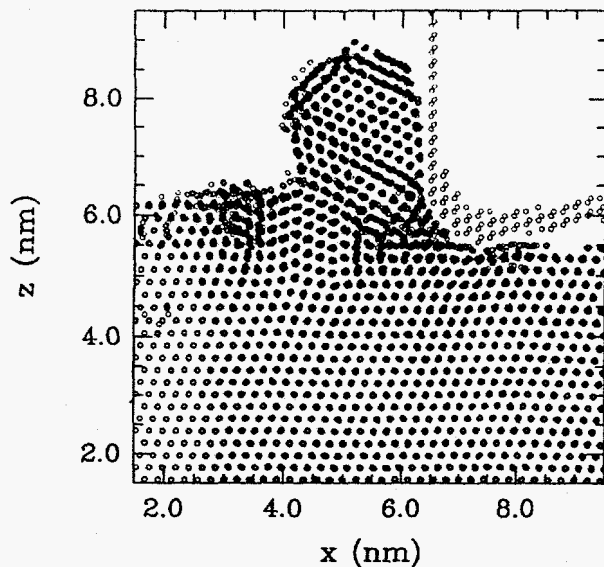
Figure 10. A projection of the state shown in Figure 8 onto the x-z plane. The copper chip remains crystalline.
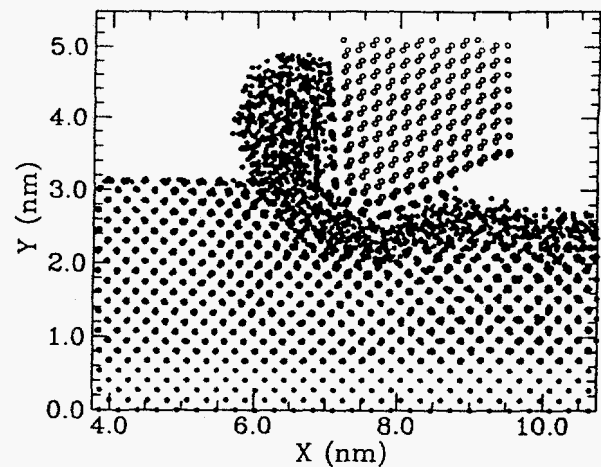
Figure 11. A projection of the system onto the x-z plane for an orthogonal cutting simulation of silicon. The silicon chip and surface transforms into an amorphous state..

ning from the disordered region in front of the tool tip to the back of the chip near the surface (i.e. the shear plane). Closer examination reveals that these are (111) planes and the intraplaner disorder reflects the presence of dislocations—these are active slip planes. A picture of the cutting process on the nanometer scale emerges: the fcc crystal wants to shear along (111) planes and the system has found it energetically favorable to dynamically reorient the crystal structure to minimize the work performed on the shear plane (i.e. the shear plane becomes an easy slip plane).

Orthogonal Cutting of the Silicon (100) Surface

Unlike copper, materials like silicon are not considered turnable with diamond tools. The diamond wears rapidly and contour accuracy is difficult to maintain. To investigate the underlying tribochemical processes we have simulated silicon machining using realistic interatomic potential models [24]. A two dimensional projection along the periodic direction from an orthogonal cutting simulation is shown in Figure 11. As yet, no wear of the diamond tool has occurred. There is a boundary layer of silicon atoms coating both rake and clearance faces of the tool, so that most of the cutting occurs between this layer and the surface. The silicon atoms in the chip and in the first few layers of newly cut surface appear to be amorphous or possibly to have melted. The temperature in the chip is comparable to the bulk melting temperature of silicon. This is in contrast to our copper simulations in which the chip remains crystalline, suggesting that during the deformation process the surface selects the state that minimizes the work done by the tool. Further details may be found in a recent paper [36].

DISCUSSION

Indentation computer experiments for the copper and silver (111) surfaces display the same qualitative behavior. For this reason we focus our discussion on silver for which a greater body of experimental information exists. In the nanoindentation experiments of Pharr and Oliver [9], an enhanced hardening effect was observed for nanoscale indents. For a 25 nm indents they observed H ~0.8 GPa, while for indents greater than 300 nm, they observed H~ 0.4 GPa. For the

simulated indent shown in Figure 10 (1.7 nm indentation), the area of contact projected onto the surface plane is about 11 nm^2 and the observed load on the tip is about 60 nN, resulting in a calculated hardness of 5.4 GPa. This value is significantly larger than the experimental value, though we note that the length scale of the simulation is an order of magnitude smaller than the experiment. The calculated hardness is reasonable if plastic deformation of the surface on the nanoscale is governed by the theoretical yield strength (Y_t) of the bulk material. We estimate this strength as $Y_t \sim G/30$, where G is the shear modulus for silver (45 GPa [33]). Hence, $Y_t \sim$ 1.5 GPa and $H_t \sim 3Y_t$ ~4.5 GPa, a value not statistically different from our calculation.

Another interesting result of the simulations is that dislocation mechanisms are not an efficient mechanism for accommodating strain on the nanometer length scale—a conclusion suggested by the nanoindentation experiments at the tens of nanometer length scale [9]. The question arises as to what length scale does dislocation mechanisms become the dominant mode of plastic deformation? The answer is intimately connected to the interplay between stored elastic energy and dislocation motion. If the system can release more elastic energy than the work required to create and move dislocations, it will do so. Both the stored elastic energy and the work required to create dislocations increase with indentation size (the minimum loop length is comparable to the radius of contact, which increases with indentation size). However, the dependence of these two energies upon indentation size is probably much different and, even though only a small fraction of the stored elastic energy will be released in a single dislocation creation event, dislocation mechanisms should become energetically favorable for sufficiently large indents. We will make this model more quantitative in our future work.

In summary, we have explicitly demonstrated in our point indentation simulations that nanoscale plasticity takes place by nondislocation mechanisms, a result suggested by nanoindentation experiments [9]. We also observe the surface to accommodate nearly the entire volume of the tip and the annealing out of plastic work as the tip is removed. In our orthogonal cutting simulation, we observe an interesting phenomenon: the system dynamically reorients the grain in front of the tool tip to minimize the work performed on the shear plane (i.e. the shear plane becomes an easy slip plane). Silicon transforms into an amorphous state which then flows plastically.

ACKNOWLEDGEMENTS

REFERENCES

1. C. Evans, CIRP Annals **40**, 571 (1991).
2. D. Tabor, The Hardness of Metals (Oxford University Press, Oxford, 1951).
3. H. Hertz, J. Reine Angew. Math. **92**, 156 (1882).
4. K.L. Johnson, Contact Mechanics (Cambridge University Press, Cambridge, 1985).
5. J. Belak and I.F. Stowers, "The Indentation and Scraping of a Metal Surface: A Molecular Dynamics Study," Proceedings of the NATO ASI on the Fundamentals of Friction, Braunlage, Germany, August (1991), I.L. Singer and H.M. Pollock eds., to be published.
6. N. Gane and F.P. Bowden, J. Appl. Phys. **39**, 1432 (1968).
7. P.J. Blau and B.R. Lawn eds., Microindentation Techniques in Materials Science and Engineering, ASTM Special Technical Publication 889 (ASTM, Philadelphia, 1986).
8. C.C. Chen and A.A. Hendrickson, J. Appl. Phys. **42**, 2208 (1971).
9. G.M. Pharr and W.C. Oliver, J. Mater. Res. **4**, 94 (1989).

10. G. Binnig, C.F. Quate, and Ch. Gerber, Phys. Rev. Lett. **56**, 930 (1986).

11. C.M. Mate, G.M. McClelland, R. Erlandsson, and S. Chiang, Phys. Rev. Lett. **59**, 1942 (1987).

12. N.A. Burnham, D.D. Dominguez, R.L. Mowery, and R.J. Colton, Phys. Rev. Lett. **64**, 1931 (1990).

13. G.S. Blackman, C.M. Mate, and M.R. Philpott, Phys. Rev. Lett, **65**, 2270 (1990).

14. N.A. Burnham, R.J. Colton, and H.M. Pollock, J. Vac. Sci. Technol. A **9**, 2548 (1991).

15. M. Salmeron, A. Folch, G. Neubauer, M. Tomitori, and D.F. Ogletree, "Nanometer Scale Mechanical Properties of Au (111) Thin Films," Preprint (1992).

16. U. Landman, W.D. Luedtke, and M.W. Ribarsky, J. Vac. Sci. Technol. A **7**, 2829 (1989).

17. U. Landman, W.D. Luedtke, N.A. Burnham, and R.J. Colton, Science **248**, 454 (1990).

18. J.B. Pethica and A.P. Sutton, J. Vac. Sci. Technol. A **6**, 2490 (1988).

19. J.R. Smith, G. Bozzolo, A. Banerjea, and J. Ferrante, Phys. Rev. Lett. **63**, 1269 (1989).

20. For a recent review, see D.W. Heermann, Computer Simulation Methods in Theoretical Physics, 2nd ed.(Springer-Verlag, Berlin, 1990).

21. M.L. Klein and J.A. Venables eds., Rare Gas Solids (Academic Press, New York, 1976).

22. M.S. Daw and M.I. Baskes, Phys. Rev. B **29**, 6443 (1984).

23. D.J. Oh and R.A. Johnson, in Atomistic Simulation of Materials: Beyond Pair Potentials, V. Vitek and D.J. Srolovitz eds. (Plenum Press, New York, 1989), p233.

24. J. Tersoff, Phys. Rev. B **37**, 6991 (1988).

25. L. Verlet, Phys. Rev. **159**, 98 (1967).

26. S. Nosé, J. Chem. Phys. **81**, 511 (1984).

27. W.G. Hoover, Phys. Rev. A **31**, 1695 (1985).

28. J.E. Lennard-Jones, Proc. Roy. Soc. Lond. **43**, 461 (1931).

29. D. Hull and D.J. Bacon, Introduction to Dislocations, 3rd. ed. (Pergamon Press, Oxford, 1984).

30. J. Belak and I.F. Stowers, "A Molecular Dynamics Model of the Orthogonal Cutting Process," ASPE annual Conference, Rochester, NY, September (1990), ASPE, P.O. Box 7918, Raleigh, NC 27695, p76.

31. For an introduction to metal cutting, see M.C. Shaw, Metal Cutting Principles (Oxford University Press, Oxford, 1984).

32. I.F. Stowers, J. Belak, D.A. Lucca, R. Komanduri, R.L. Rhorer, T. Moriwaki, K. Okuda, N. Ikawa, S. Shimada, H. Tanaka, T.A. Dow, and J.D. Drescher, "Molecular Dynamics Simulation of the Chip Formation Process in Single Crystal Copper and Comparison with Experimental Data," ASPE Annual Conference, Santa Fe, NM, October (1991), ASPE, P.O. Box 7918 Raleigh, NC 27695, p100.

33. C.J. Smithells, ed. Metals Reference Book, 5th ed. (Butterworths, London, 1976).

34. D.W. Brenner, Phys. Rev. B **42**, 9458 (1990).

35. D.W. Brenner, J.A. Harrison, C.T. White, and R.J. Colton, Thin Solid Films **206**, 220 (1991).

36. Boercker, D.B, J. Belak, I.F. Stowers, R. Donaldson, and W. Siekhaus 1992. "Simulation of Diamond Turning of Silicon Surfaces," In Proceedings of the American Society for Precision Engineering Annual Conference (Grenelefe, FL, October 18-23). ASPE, PO Box 710826, Raleigh, NC 27605-0826.